Carbohydrate Polymers 102 (2014) 47–54

Contents lists available at ScienceDirect

Carbohydrate Polymers

journal homepage: www.elsevier.com/locate/carbpol

Immunostimulatory activities of β-D-glucan from *Ganoderma Lucidum*

Jianguo Wang*, Yahong Yuan, Tianli Yue

College of Food Science and Engineering, Northwest A&F University, Yangling, Shaanxi 712100, China

ARTICLE INFO

Article history:
Received 4 March 2013
Received in revised form 14 October 2013
Accepted 29 October 2013
Available online 6 November 2013

Keywords:
Ganoderma Lucidum
β-Glucan
Anti-inflammation
Cytokines
Signal pathways

ABSTRACT

A water-insoluble β-(1→3)-D-glucan (GLPs) with few branches at C-6 and C-2 positions was extracted from the fruit body of *Ganoderma Lucidum* by 1 M NaOH at 40 °C. By the striking inhibition of NO and TNF-α production, GLPs showed significant anti-inflammation activity against LPS induced Raw 264.7 cells. Results of RT-PCR revealed the down regulation of iNOS and TNF-α mRNA gene expression. GLPs severely inhibited the phosphorylation of IκBα and JNK1/2, while the ERK1/2 and p38 were not apparently affected by GLPs. The neutralizing antibodies against dectin-1 and TLR-4, respectively, did not affect GLPs-mediated inhibition of NO production. But neutralizing of TLR2 affected the inhibition of NO. All of these results revealed that GLPs can inhibit the inflammation of Raw 264.7 cell induced by LPS at least partially attributed to the blocking of NF-κB and JNK MAPK, and TLR2 plays a major role in GLPs anti-inflammation activity.

1. Introduction

Inflammation, beneficial response of the body immune system, is a response to injury, infection, and stress. Lipopolysaccharide (LPS) plays a key role in the initiation of inflammation by activating macrophages, leading to the high production of Nitric oxide (NO), Tumor necrosis factor-α (TNF-α) and interleukins (ILs) (Chelvarajan et al., 2006; Gerber & Mosser, 2001). As well reported, NO and TNF-α were two key molecules in the pro-inflammation activity of murine macrophage (John, Xie, & Nathan, 1997; O'Shea & Murray, 2008). TNF-α resulted in the increased number of macrophage that had enhanced microbicidal or tumoricidal capacity and secreted high levels of pro-inflammatory cytokines such as IL-1, IL-6 and IL-12. NO is synthesized by nitric oxide synthases (NOS), which is found in various isoforms, such as neuronal NOS (nNOS), endothelial NOS (eNOS), and inducible NOS (iNOS). Among these NOS, iNOS expression is closely involved in nuclear factor κB (NF-κB) signal pathway that is otherwise induced by various effectors, such as LPS (Hwang et al., 2011). Except for NF-κB signal pathway, MAPKs (mitogen-activated protein kinase) including ERK, JNK and p38 pathways also are well demonstrated to be responsible for the LPS-induced activation of macrophage to produce inflammatory cytokines and chemokines (Zhang & Ghosh, 2001). The pro-inflammatory cytokines that are produced by classically activated macrophages are an important component of host defense, but they can cause extensive damage to the host (Liao & Lin, 2012), ranging from direct cellular cytotoxicity (Chung, Pae, Choi, Billiar, & Kim, 2001) to damage of components leading to mutagenesis (Ahn et al., 2005). Therefore, reagents possess anti-inflammatory activity is of great pharmacological interest.

Glucans are polymers of glucose that are widely distributed throughout the biosphere. Specifically, β-glucan found in the cell walls of plants, bacteria and fungi are well known to possess significant and wide biological and physiological activities, including antitumor, antioxidant, anticoagulant, antifungal and immunomodulating activity (Brown & Gordon, 2005; Lacchini, Davies, Mackintosh, & Walker, 2006; Leung, Liu, Koon, & Fung, 2006; Lin, Liang, Lee, & Chiang, 2005). In this work, we reported one almost linear water insoluble β-(1→3)-D-glucan with relatively low molecular weight, coded as GLPs, obtained from the fruit body of *Ganoderma Lucidum*. This glucan significantly inhibited the LPS-induced inflammation against Raw 264.7 cells. This work demonstrated the anti-inflammation activity of GLPs and clarified the signal transduction pathways.

2. Materials and methods

2.1. Materials

Dried *Ganoderma lucidum* was kindly provided as a gift by *Longyan* College in Fujian, China. The fruit body was powdered, and then defatted by using a Soxhlet extractor with ethyl acetate for 8 h and then with acetone for 8 h. The resultant residue was immersed in 0.9% NaCl solution at 95 °C, respectively, and then stirred three times for 24 h to remove the water-soluble parts. The residue mentioned above was extracted with 1 M NaOH solution for

* Corresponding author. Tel.: +86 29 88092486; fax: +86 29 88092486.
E-mail addresses: wjg5118@nwsuaf.edu.cn, wjg5118@yeah.net (J. Wang).

0144-8617/$ – see front matter © 2013 Elsevier Ltd. All rights reserved.
http://dx.doi.org/10.1016/j.carbpol.2013.10.087

8 h at 40 °C. The resulting extract was centrifuged at 7000 rpm and then the supernatant was neutralized by acetic acid. The deposition was collected and washed with distilled water ten times, then lyophilized to get a white powder, coded as GLPs. To get a more purified sample, the polysaccharide was dissolved in Dimethyl sulfoxide (DMSO, Sigma–Aldrich) with stirring at 25 °C overnight and then centrifuged to obtain the supernatant. The supernatant was dialyzed (regenerated cellulose tubing: Mw cut-off 8000, USA) with distilled water for one week to get a white precipitate, which was lyophilized to get the pure white powder and the final yield was 7.6%. GLPs was dissolved in DMSO to prepare an accurate 5 mg/ml solution and kept in room temperature, the concentrations needed in cell culture was diluted from the original 5 mg/mL solution by the culture medium.

2.2. Characterization of GLPs

Infrared spectra of the samples were recorded with Nicolet Fourier transform infrared (FTIR) spectrometer (Spectrum One, Thermo Nicolet Co., Madison, WI, USA) in the range 4000–400 cm^{-1} using the KBr disk method.

2.3. Determination of monosaccharide and D or L-configuration

The monosaccharide composition was analyzed by alditol acetates derivatives of the samples using Gas chromatography (GC) described by Yasuyuki et al. (Tezuka, Imai, Oshima, & Chiba, 1987). GC analysis was carried out with an Agilent 6820 gas chromatograph system (Agilent, Palo Alto, CA, USA) equipped with a flame ionization detector using a DB-5MS capillary column (30 m × 0.32 mm × 0.25 μm) programmed from 180 °C to 220 °C at 4 °C/min and held at 220 °C for 30 min. The injection volume was 3 μL, the carrier gas was high-purity nitrogen.

The polysaccharide was methanolized with 0.625 M methanolic HCl, treated with 0.625 M (+)-2-butanolic-HCl. After butanolysis for 18 h at 80 °C, the solution was neutralized with Ag_2CO_3, the supernatant concentrated, and dissolved in 50 ml. Thereafter we added 50 ml of bis(trimethylsilyl) trifluoro acetamide (Sigma) and kept the solution for 30 min at room temperature. The butanolyzed and trimethylsilylated derivatives were analyzed on a DB-5 GLC column. The temperature program was iso-thermal at 130 °C followed by 2 °C/min gradient up to 250 °C.

2.4. Glycosidic linkage analysis

GLPs were methylated according to Hakomori followed by hydrolysis (Hakomori, 1964), reduction and acetylation of the partially methylated alditols to further investigate their structural characteristics, especially the glycosidic linkage types. The polysaccharide samples were first methylated by CH_3I, and then extracted with $CHCl_3$. These extracts were washed with distilled water to remove the unmethylated water-soluble polysaccharide. The methylated polysaccharide was hydrolyzed in 12 M H_2SO_4 at 20 °C for 1 h, followed by 2 M H_2SO_4 at 90 °C for 2 h, and then acetylated with acetic anhydride (Ac_2O) in pyridine at 90 °C for 3 h. The samples were directly hydrolyzed and acetylated. Gas chromatography–mass spectrometry (GC/MS) was carried out on a GCT system (Macro-Mass, Waters, USA) with a capillary GC column (HP-5MS, 30 m × 0.32 mm ID × 0.25 m, Agilent, USA) using N_2 as carrier gas. The oven temperature was set to increase from 180 °C to 220 °C at a rate of 4 °C/min and the detector temperature was set at 250 °C.

2.5. Molecular characteristics

A size-exclusion chromatograph combined with multi-angle laser light scattering (SEC-LLS) combined with concentration detectors such as UV and differential refractive index (DRI) has been demonstrated to be a convenient method for characterization and analysis of highly poly-disperse polymer system (Wang, Zhang, Yu, & Cheung, 2009). SEC-LLS measurements of GLPs were carried out on SEC combined with LLS, a P100 pump (Thermo separation products, San Jose, CA, USA) equipped with a column of G4000HXL in DMSO at 25 °C was used as the SEC instrument. A differential refractive index detector (RI-150, Thermo Separation Products, San Jose, CA, USA) was simultaneously connected. The carrier solution was DMSO. The solvents and polysaccharide solutions were purified by a 0.2 μm filter and degassed before use. The injection volume was 200 μL with a concentration of 2 mg/mL for the sample, and the flow rate was 0.5 mL/min. Astra software (version 4.90.07) was utilized for data acquisition and analysis.

2.6. Reagents and antibodies

RPMI-1640 medium (glutamine, high glucose), penicillin, streptomycin, and fetal bovine serum (FBS) were purchased from Lonza (Walkersville, MD, USA). LPS from *Escherichia coli* were purchased from Sigma. Antibodies were obtained from the following sources: rabbit polyclonal anti-Iκ-Bα-mAb, rabbit polyclonal anti-phospho-ERK1/2, rabbit polyclonal anti-phospho-JNK1/2, and rabbit polyclonal antiphospho-p38 (BD Biosciences). Mouse monoclonal anti β-actin, monoclonal antibody against TLR2/CD282, monoclonal antibody against TLR4/CD284 and mouse monoclonal antibody against Dectin-1/CLEC7A were obtained from company (Cell Signaling Technology). The water used in all experiments was ultrapure by a Milli-Q water purification system from Millipore. All chemicals and reagents used in this work were analytical grade.

2.7. Cell culture

Raw 264.7 cells (American Type Culture Collection) were maintained in RPMI-1640 supplemented with penicillin (100 units/ml), streptomycin (100 μg/ml), and 10% heat-inactivated FBS at 56 °C for 30 min. Cells were harvested by cell scraper, followed by centrifugation and seeding into the culture flask or plates, which was incubated at 37 °C under a humidified atmosphere of with 5% CO_2.

2.8. Macrophage proliferation and anti-inflammation assay

Raw 264.7 cells were cultivated in a 96-well microplate (1×10^6 cells/well, in a volume of 100 μL; obtained from ATCC) and incubated in RPMI-1640 medium containing 10% FBS with 100 μL of the GLPs at different concentrations (0, 5, 20, 50 and 100 μg/mL) with or without the addition of LPS (1 μg/mL). Each concentration was tested in triplicate. Cells were incubated at 37 °C in a 5% CO_2 incubator. After 24 h, the WST-1 reagent was used to determine the proliferation of macrophage cells. Absorbance at 450 nm was determined by spectrophotometer. The absorbance (A) was translated into macrophage proliferation ratio (%) = $(A_t/A_c) \times 100$, where A_t and A_c were the absorbance of the test group and control group (culture medium treated group), respectively.

The anti-inflammation activity of the polysaccharides was determined on the basis of NO production in macrophage culture supernatants, and the NO concentration was measured using the Griess reaction as described by Green et al. (Green et al., 1982). Raw 264.7 cells were cultivated in a 96-well microplate (1×10^5 cells/well, in a volume of 100 μL) and incubated for 24 h at 37 °C in a 5% CO_2 incubator. The cultured cells were treated with polysaccharide solutions (100 μL) at concentrations ranging from 5 to 100 μg/mL mixed with LPS solution (1 μg/mL), which was also used as a positive control (labeled as “LPS” in the figures). Culture medium treated groups without the presence of LPS and GLPs were as negative control (labeled as “control” in the

figures). After incubating for 24 h at 37 °C, the cultured cell supernatant (100 μL) was mixed with an equal volume of Griess reagent (1% [w/v] sulfanilamide and 0.1% [w/v] N-[1-naphthyl] ethylenediamine hydrochloride in 2.5% [v/v] phosphoric acid) and incubated at room temperature for 10 min. The absorbance was measured at 540 nm using a microplate reader. NO production from the Raw 264.7 cells was calculated with reference to a standard curve that was obtained with $NaNO_2$ (1–200 μM in the culture medium).

2.9. TNF-α assays by ELISA

Raw 264.7 cells (1×10^6 cells/well) were seeded into 24-well plates and incubated for 24 h before stimulation. At the end of preincubation, cells were rinsed with PBS and, the medium was exchanged to RPMI with 1% FBS. The cells were exposed to LPS (1 μg/ml) with and without of GLPs (100 μg/ml). After 24-h stimulation, the conditioned medium was collected and centrifuged, and the TNF-α level in the supernatant were assessed using an ELISA kit (Thermo Scientific) according to the manufacturer's instructions.

2.10. RT-PCR for transcriptional analysis

To investigate the levels of mRNA gene expression of iNOS and TNF-α, Raw 264.7 cells (1 mL, 1×10^6 cells/well) in 24 well plate were treated with LPS (1 μg/mL) combined with different concentrations of polysaccharides (0, 5, 20, 50 and 100 μg/mL) at 37 °C in the presence of 5% CO_2 for 18 h. The RNA was extracted from the cells using the TRIzol reagent (Invitrogen, Carlsbad, CA, USA) according to the manufacturer's protocol and kept at −80 °C until use. The concentration of the extracted RNA was measured via a spectrophotometer before constructing cDNA with an oligo-(dT)20 primer and Superscript III RT (Invitrogen, Carlsbad, CA, USA). The resulting cDNA was amplified by PCR using GoTaq Flexi DNA Polymerase (Promega, Madison, WI, USA). Reverse transcriptase amplification was conducted with an initial denaturation at 94 °C for 3 min and 30 cycles of denaturation (94 °C for 30 s), annealing (56 °C for 40 s) and extension (72 °C for 1 min) followed by a final extension step at 72 °C for 10 min. The products of RT-PCR were separated by gel electrophoresis using 1% agarose gel stained with ethidium bromide, and the gels were viewed under UV transillumination. The sequences of the primers used in this experiment were: 5′-CCCTTCCGAAGTTTCTGGCAGCAGC-3′ (forward) and 5′-GGCTGTCAGAGCCTCGTGGCTTTGG-3′ (reverse) for iNOS, 5′-ATGAGCACAGAAAGCATGATC-3′ (forward) and 5′-TACAGGCTTGTCACTCGAATT-3′ (reverse) for TNF-α, 5′-TACCTGG-TAGAAGTGATGCC-3′ (forward) and 5′-TAAAACGCAGCTCAGTAAC-AGTCCG -3′ (reverse) for β-actin.

2.11. Western blotting

Cellular lysates were prepared by suspending 1.5×10^6 cells in 100 μl of lysis buffer (137 mM NaCl, 15 mM EGTA, 0.1 mM sodium orthovanadate, 15 mM $MgCl_2$, 0.1% Triton X-100, 25 mM MOPS (4-morpholinepropanesulfonic acid), 100 μM phenylmethylsulfonyl fluoride, and 20 μM leupeptin, adjusted to pH = 7.2), disrupted by sonication and extracted at 4 °C for 30 min. Whole cell extracts (30 μg protein/lane) were separated on 10% SDS-polyacrylamide gels. The separated proteins were electrophoretically transferred onto nitrocellulose membranes. After blocking with 5% (w/v) BSA in TBS (10 mM Tris–HCl (pH 8.0), 150 mM NaCl) containing 0.1% Tween 20 at room temperature for 1 h, the membranes were then incubated with appropriate specific primary antibody (anti-iNOS, 1:8,000; anti-ERK1/2, 1:1,000; anti-JNK1/2, 1:1,000; anti-p38, 1:1,000; anti-Iκ-Bα-mAb, 1:1000; anti-β-actin, 1:20,000) overnight at 4 °C. The reactive bands were visualized with an HRP-conjugated secondary antibody (1:20,000; Santa Cruz Biotechnology) via ECL Western blot detection reagents on a Light Capture II according to the manufacturer's instructions (Amersham Biosciences).

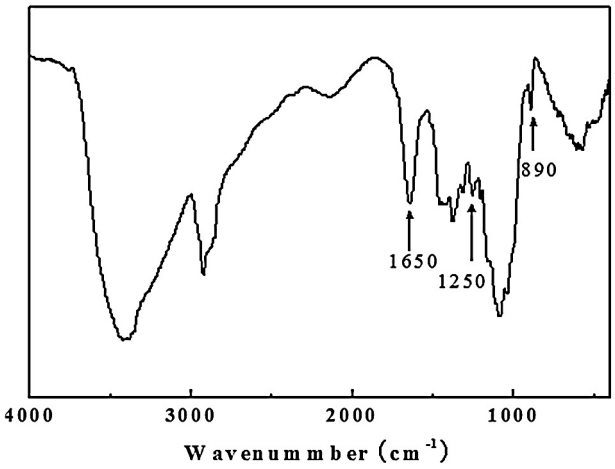

Fig. 1. FTIR spectra of GLPs.

2.12. Anti-dectin1 and anti-TLR2/4 antibody neutralization assay

RAW 264.7 cells were seeded at a density of 1×10^6 cells/ml in 24-well plate. After a 24 h pre-incubation, the cells were incubated with 20 μg/ml monoclonal antibodies against murine Dectin-1/CLEC7A, TLR2/CD282 and TLR4/CD284 for 30 min at 37 °C. LPS (1 μg/ml) and GLPs (5–100 μg/ml) were then added into the medium with 1% FBS and incubated for another 24 h. The supernatants were finally collected, and the concentration of NO was measured by the method described above.

2.13. Statistical analysis

All experiments were performed in triplicate ($n = 3$). Data were presented as the mean value with standard deviation. Statistical differences were tested by Student's t test, a one-way analysis of variance (ANOVA), and Duncan's multiple-range test. The critical p value was set at 0.05; a probability value of $p < 0.05$ was considered to be statistically significant.

3. Results and discussion

3.1. Chemical structure

The FTIR spectrum of GLPs was shown in Fig. 1. GLPs exhibited the characteristic FTIR absorption of the polysaccharide at 1250 and 1650 cm^{-1}, which should be attributed to the deviational vibration of C—H and —OH groups, respectively. Meanwhile, GLPs exhibited the significantly absorption peak at 890 cm^{-1}, which is the characteristic absorption peak of β configuration of polysaccharides. Monosaccharide and absolute configuration analysis further confirmed that GLPs was only composed of D-glucan, indicating GLPs was β-D-glucan.

3.2. Glycosidic linkage analysis

The nature of glycosidic linkage of GLPs was elucidated by methylation analysis using GC–MS. GLPs consists only glucan as determined above. Fig. 2 shows the total ion current (TIC) chromatograms and the electron impact profile of the partially methylated alditol acetate (PMAA) range of m/z 80–260 and its key ions. As we can see, only one major peak at 10.467 min was

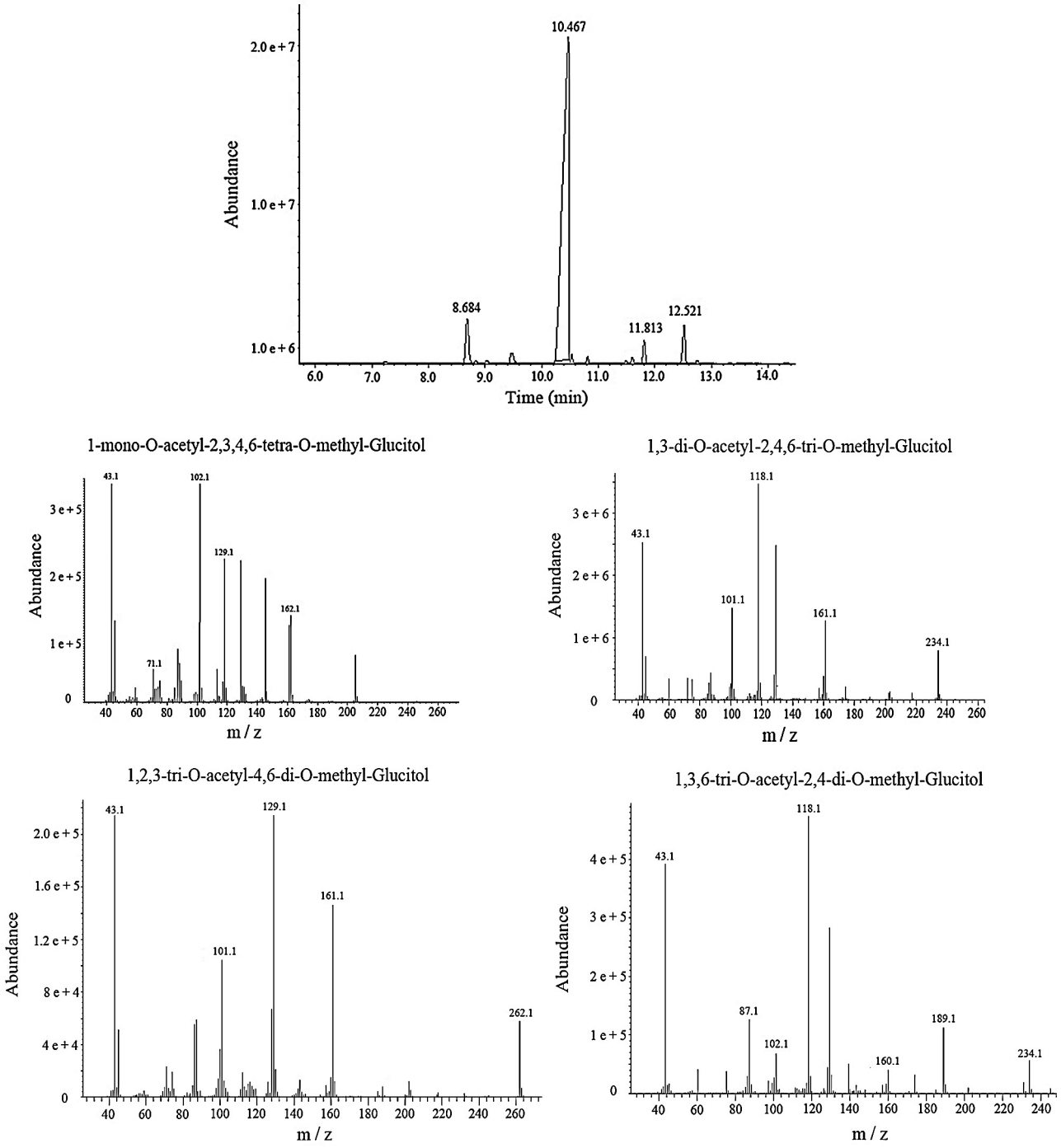

Fig. 2. GC chromatograms and the electron impact profile of each PMAA determined by MS.

determined in GC spectra and the molar ration was 91.166%. Meanwhile, three other small peaks were observed at 8.648, 11.813 and 12.521 min with the molar ratio of 4.395%, 1.309% and 3.131%, respectively. According to key characteristic ions of the mass spectra, the major residue at 10.467 min was assigned to 1,3-di-O-acetyl-2,4,6-tri-O-methyl-glucitol, indicating the main chain of GLPs was β-(1→3)-D-glucan. The terminal residue was detected at 10.467 min in a ratio of 4.395%. Peak of GC spectra at 12.521 min was assigned to 1,3,6-tri-O-acetyl-2,4-di-O-methyl-glucitol, and the ratio of this 1, 3→6) residues was 3.131%. Meanwhile, the smallest peak at 11.813 min was assign to 1,2,3-tri-O-acetyl-4,6-di-O-methyl-glucitol, demonstrating the existing of 1, 2→3) residues. Based on the results above, the backbone of GLPs was mainly linked by β-(1→3) linked glucuronosyl residues with few branches occurrence at C-6 and C-2 position, and the branching ration at C-6 and C-2 were 3.131% and 1.309%, respectively. All the structural date above elucidated that GLPs was almost linear β-(1→3)-D-glucan with few branch at C-6 and C-2 positions.

3.3. Molecular characteristics

SEC-LLS, as an absolute method, is a convenient method for the determination of the true molecular mass and its distribution. The SEC patterns of GLPs in DMSO analyzed by the LLS (detector

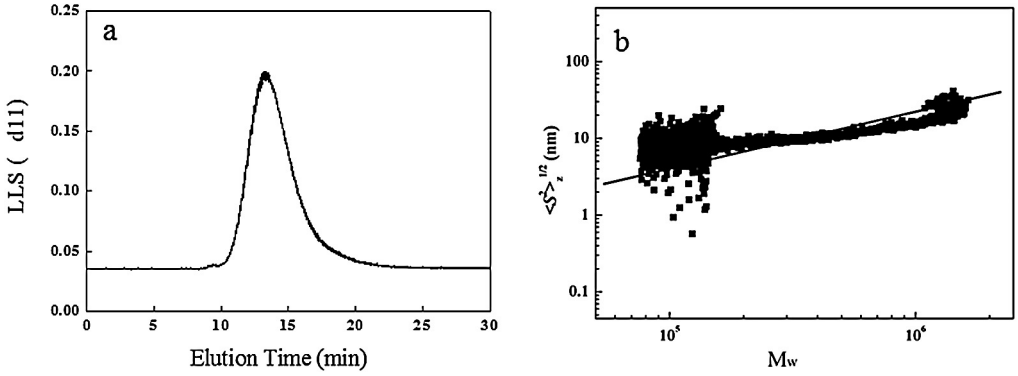

Fig. 3. SEC patterns of GLPs (a) from LLS (detector 11) and dependence of $\langle S^2\rangle_z{}^{1/2}$ on M_w for GLPs (b) in DMSO at 25 °C.

$d_{11} = 90°$) at 25° C were shown in Fig. 3a. obviously, there was one single peak with good symmetry for GLPs detected by LLS. The weight average molecular mass (M_w) of GLPs was 13.3×10^4. From the SEC chromatogram detected by LLS, we could obtain the M_w and $\langle S^2\rangle_z{}^{1/2}$ values of numberless fractions. The M_w – $\langle S^2\rangle_z{}^{1/2}$ relationship from many experimental points in the SEC can give conformation parameters. From data of M_w and $\langle S^2\rangle_z{}^{1/2}$, the power law describing the relationship between M_w and $\langle S^2\rangle_z{}^{1/2}$ ($\langle S^2\rangle_z{}^{1/2} = K M_w\alpha$) can be created. The chain conformation of the polymer in solution can be estimated by the value of exponent (α). Usually, the α value is 0.3 for globular shape, 0.5–0.6 for flexible chain conformation in good solvent, and 0.6–1 for a semi-flexible or stiff chain (Picton, Bataille, & Muller, 2000). The log-log plots of $\langle S^2\rangle_z{}^{1/2} \propto M_w\alpha$ for GLPs in DMSO was also shown in Fig. 3b, the α value for GLPs was 0.47, indicating that the glucan existed as a flexible chain conformation.

3.4. Cytotoxic effect of GLPs and NO production

As shown in Fig. 4a, the cytotoxic effects of GLPs on the proliferation of Raw 264.7 cells were evaluated at different concentration of 5–100 μg/mL. The GLPs alone did not considerably affect the proliferation of Raw 264.7 cells, suggesting that the polysaccharides were not toxic to Raw 264.7 cells over the concentration range tested in this study. The same situations were observed in the GLPs combined LPS groups, and the final concentrations of LPS in the "GLPs + LPS" groups were all 1 μg/ml combined with different concentration of GLPs from 5 to 100 μg/mL. The proliferations in all testing groups were comparable to that of the control group (culture medium treated group), indicating GLPs showed no toxic effects against Raw 264.7 cells in our measurement.

Fig. 4b shows the NO production of GLPs stimulated Raw 264.7 cells. As we can see, the NO production of GLPs alone treated macrophage were quite comparable to that of culture medium treated group (control group), indicating that GLPs didnot show any pro-inflammation effect and didnot induce the NO production against Raw 264.7 cells. As to the positive control group, LPS treated without the presence of GLPs, the final NO concentration in the culture medium was 56 μM/mL. After adding different concentrations of GLPs, the NO production induced by LPS were decreased in a dose dependent manner, which decreased to 42, 23, 14 and 11 μM/ml in the presence of GLPs at the final concentration of 5, 20, 50 and 100 μg/ml, respectively, indicating the apparently inhibition to the LPS induced inflammation. The inhibition ratios of the GLPs were highly significant (20–100 μg/mL) compared to LPS group ($p \leq 0.01$). At the concentration of 100 μg/ml GLPs combined with 1 μg/ml of LPS, the NO production was quite comparable to the culture medium, demonstrating the almost totally inhibition of the LPS-induced inflammation.

3.5. GLPs suppressed the TNF-α production in the cell culture medium

The final TNF-α concentration in the cell culture mediums was tested by ELISA kits according to the procedure of manufacture. As shown in Fig. 4c, LPS without GLPs treatment induced substantial TNF-α production in Raw 264.7 cells, and GLPs suppressed TNF-α production similarly in a dose dependent manner with inhibition around 76% at the concentration of 100 μg/ml under 24 h stimulation. This result again confirmed the significant inhibition of inflammation of GLPs induced by LPS against Raw 264.7 macrophage.

3.6. Effects of anti-dectin-1 and anti-TLR antibodies on inhibition of NO production

Denctin-1 has been extensively identified to be involved in mediating the biological effects β-glucan as the major receptor, which is expressed at high levels on macrophages and neutrophils, and to a lesser extent on dendritic cells and a subpopulation of T cells (Brown et al., 2003). Other pattern-recognition receptors (PRRs) detect molecular signature of microbes and initiate immune responses to infection are TLRs. TLRs signal via a conserved pathway to induce innate response genes. Dectin-1 is known to synergize with TLR2 to induce TNF-α and IL-12 through phosphorylation of the membrane proximal tyrosine in the cytoplasmic domain (Akira, Tokeda, & Kaisho, 2001; Rogers et al., 2005). To verify which pattern-recognition receptor did GLPs involve in the inhibition of the LPS-induced NO production, we used anti-Dectin-1 mAb, anti-TLR2 mAb and anti-TLR4 mAb to neutralize Dectin-1, TLR-2 and TLR 4, respectively. The NO productions as mentioned above were detected subsequently. In our study, productions of NO were not affected by the neutralization of Dectin-1 and TLR-4, while the productions of NO were apparently affected treated with the anti-TLR2 mAb. As shown in Fig. 4d, after the neutralization of TLR-2, the NO production of Raw 264.7 cells treated with LPS in the presence of varies concentration of GLPs significantly decreased while the effects of the neutralization of TLR-4 and Dectin-1 did not affect the NO production (Data of the neutralization of TLR-4 and Dectin-1 were not shown here), which indicated the major roles of TLR2 plays in the LPS-induced inflammation of macrophage. The final concentration in the culture mediums was 27, 22, 18, 15 μM/mL in a concentration dependent manner of GLPs. The NO production of Raw 264.7 cells treated only with GLPs was 12 μM/mL, which was comparable to that of the negative control as showed in Fig. 4d.

3.7. RT-PCR for iNOS and cytokine gene expression

As we know, iNOS and TNF-α were synthesized by translation of the corresponding mRNA in the cytoplasm. As proved, stimulation

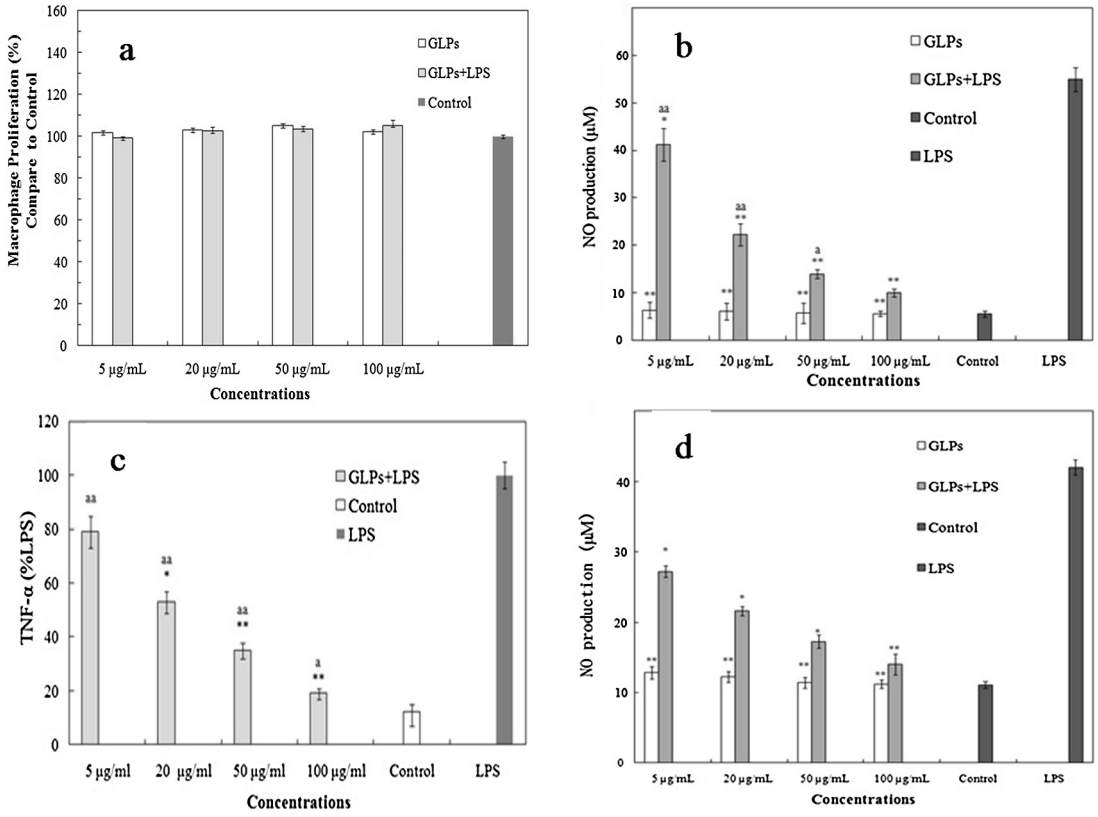

Fig. 4. Proliferation of GLPs and GLPs + LPS against Raw 264.7 cells (a). NO production of GLPs and GLPs + LPS against Raw 264.7 macrophage cells (b). TNF-α production of GLPs and GLPs + LPS against Raw 264.7 macrophage cells (c). NO production of GLPs and GLPs + LPS against Raw 264.7 macrophage cells after the incubation with 20 μg/ml monoclonal antibodies against murine TLR2/CD282 (d). Each value represents the mean value of three independent experiments. "*": $p \leq 0.05$ versus LPS; "**": $p \leq 0.001$ versus LPS; "a": $p \leq 0.05$ versus Control; "aa": $p \leq 0.001$ versus Control.

of macrophages with LPS induces iNOS protein expression, resulting in the conversion of L-arginine to NO and L-citrulline (Brown, 2003). It is also well known that activated macrophages can inhibit the proliferation of tumor cell through the release of TNF-α, which is responsible to activate the macrophage (Hou, Chen, Huang, & Jeng, 2006). To clarify how GLPs decrease the NO and TNF-α production, iNOS mRNA and TNF-α mRNA expression were examined by RT-PCR analysis. As shown in Fig. 5, the iNOS and TNF-α mRNA gene expression showed that after the treatment of GLPs and LPS for 24 h without the addition of GLPs, cells treated with 1 μg/ml LPS for 24 h expressed high level of iNOS and TNF-α mRNA than the culture medium treated group. These two mRNA can hardly be detected in the culture medium treated cell. After adding varies concentrations of GLPs, the LPS-induced iNOS and TNF-α mRNA production were significantly inhibited in a dose dependent manner. GLPs showed the highest inhibition in both of the two pro-inflammation cytokines at the highest concentration tested (100 μg/ml), the expression of iNOS and TNF-α mRNA were also hardly detected in this concentration of GLPs. These results almost followed a tendency similar to that of NO release, which suggested that GLPs might suppress the excessive inflammation of Raw 264.7 cells.

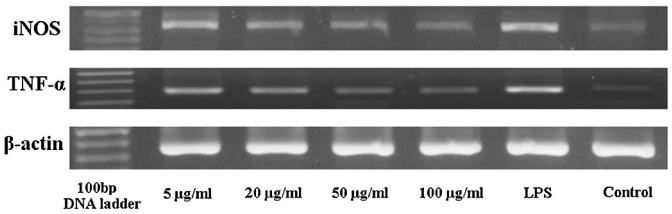

Fig. 5. iNOS and TNF-α mRNA production of GLPs at different concentration combined with LPS against Raw 264.7 macrophage cells.

3.8. GLPs is an inhibitor of LPS-induced phophorylation of Iκ-Bα in Raw 264.7 cells

Further Western blotting investigation was performed to elucidate NF-κB in the Raw 264.7 cells, which is also well known to be important in the induction of iNOS by LPS (Kim et al., 2004). NF-κB regulates the transcription of such gene as iNOS and macrophage-related cytokines. The NF-κB dimer (p65/p50) in resting cells is held in the cytosol by interaction with Iκ B inhibitory proteins. After its exposed to pro-inflammatory stimuli, Iκ B is phosphorylated by Iκ B kinase ubiquitinated and then degraded, and the degradation and phosphorylation of Iκ-B are necessary to release NF-κB from the cytoplasmic NF-κB/Iκ-Bα complex to allow its subsequent translocation to the cell nucleus. So the low content of the Iκ-Bα (a degraded form of Iκ-B) reflects the activation of the NF-κB signal pathway. Fig. 6 demonstrates the high expression of Iκ-Bα in the culture medium and GLPs treated Raw 264.7 cells. The Iκ-Bα in the LPS stimulated group was only 0.49 compared to that of the culture medium treated cells, while the expression in GLPs combined LPS were 0.91, 0.90 and 0.94 at the concentration from 20 to 100 μg/ml, these results indicated the GLPs inhibited the degradation of Iκ-B and blocked the NF-κB pathway, which might resulted in the inhibition of the inflammation against the Raw 264.7 cells induced by LPS.

3.9. GLPs is an inhibitor of LPS-induced phophorylation of JNK in Raw 264.7 cells

Multicellular organisms have three well-characterized subfamilies of ERK, JNK and p38 MAPKs that control a vast array of

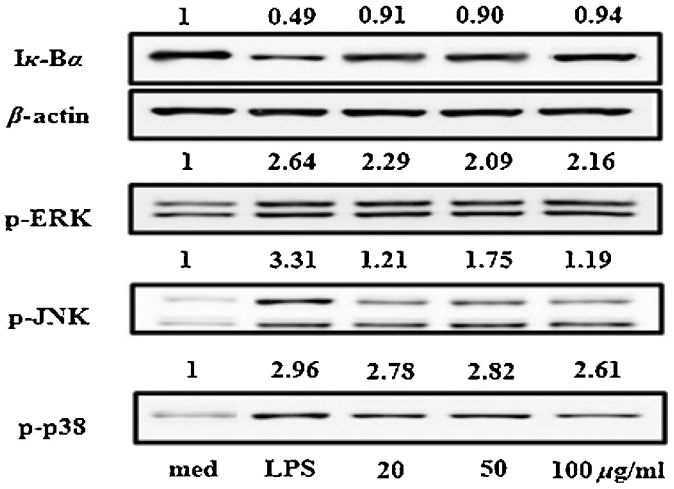

Fig. 6. GLPs interfered with MAPK signaling pathways and enhanced Iκ-Bα nuclear translocation and NF-κB transcription activity.

physiological processes including inflammation. These enzymes are regulated by a characteristic phosphorylation system in which a series of three protein kinases phosphorylate and activate one another (Gary & Lapadat, 2002). As we know, ERK, JNK and p38 MAPK pathways are involved in LPS stimulation of Raw 264.7 cells (Aballay, Drenkard, Hilbun, & Ausubel, 2003; Chan & Riches, 2001). The phosphorylation and activation of the MAPKs are involved in the iNOS and TNF-α activation flowing by the inflammation of the macrophage. To investigate whether the ERK, JNK and p38 MAPK pathways can be blocked by GLPs, we measured the phosphorylation of the ERK, JNK and p38 by Western blotting. As we can see from Fig. 6, treatment with GLPs significantly inhibited JNK phosphorylation, the JNK phosphorylation of LPS treated without the presence of GLPs was 3.31 folds higher than those of culture medium treated cells, and with the presence of GLPs treatments at different concentration from 20 to 100 μg/ml with the same dose of LPS (1 μg/ml) were only 1.21, 1.75 and 1.19 folds higher than the culture medium treatment, respectively, much lower than the LPS treated without the addition of GLPs. The dose dependent manner in the inhibition of the phosphorylation of JNK were not as regular as the inhibition of the production of NO and TNF-α, partially may because of the complicate intracellular environment. On the other hand, ERK and p38 MAPK phosphorylations were not significantly affected by GLPs. Both the two MAPKs showed much higher expression stimulated by LPS in absence and presence of GLPs, indicating GLPs hardly affected the LPS-induced activation though the ERK and p38 MAPKs pathways. These results were in consistent with the report of Kim (Kim et al., 2004), indicating the JNK might be more reliable to the anti-inflammation according to the case of GLPs.

4. Conclusions

On the basis of the results mentioned above, the linear water insoluble β-(1→3)-D-glucan with few branch at C-6 and C-2 positions extracted from *Ganoderma Lucidum* exhibited significant inhibition of inflammation induced by LPS against Raw 264.7 cells in a dose dependent manner. This glucan decrease the NO production, at least partially, via blocking NF-κB and the inhibiting the phosphorylation of JNK MAPK signal pathways. Meanwhile, TLR2 may be the major pattern recognition receptors on Raw 264.7 cells membrane for GLPs to affect the inflammation induced by LPS. However, more further study are needed to clarify the detailed role of GLPs played in the NO production dependent on TLR2, and the upstreaming and downstreaming JNK MAPK signaling pathways, transcription factors and the receptors involved in the anti-inflammation mechanism will be further studied in our future work.

Acknowledgements

We gratefully acknowledge the financial support of National Natural Science Foundation of China (31071550, 31171721), National "12th-Five-Year Plan" scientific and technological schemes support (2012BAD31B01, 2012BAK17B06), Research Fund for the Doctoral Program of Higher Education of China (20130204120041) and a doctoral research fund of Northwest A&F University (Z109021107).

References

Aballay, A., Drenkard, E., Hilbun, L. R., & Ausubel, F. M. (2003). Caenorhabditis elegans innate immune response triggered by *Salmonella enterica* requires intact LPS and is mediated by a MAPK signaling pathway. *Current Biology*, *13*, 47–52.

Ahn, K. S., Noh, E. J., Zhao, H. L., Jung, S. H., Kang, S. S., & Kim, Y. S. (2005). Inhibition of inducible nitric oxide synthase and cyclooxygenase II by *Platycodon grandiflorum* saponins via suppression of nuclear factor-kappaB activation in RAW 264.7 cells. *Life Sciences*, *76*, 2315.

Akira, S., Tokeda, K., & Kaisho, T. (2001). Toll-like receptors: Critical proteins linking innate and acquired immunity. *Nature Immunology*, *2*, 675–680.

Brown, G. C. (2003). NO says yes to mitochondria. *Science*, *299*, 838–839.

Brown, G. D., & Gordon, S. (2005). Immune recognition of fungal β-glucans. *Cellular Microbiology*, *7*, 471–479.

Brown, G. D., Herre, J., Williams, D. L., Willment, J. A., Marshall, A. S. J., & Gordon, S. (2003). Dectin-1 mediates the biological effects of β-glucans. *Journal of experimental medicine*, *197*, 1119–1124.

Chan, E. D., & Riches, D. W. H. (2001). IFN-γ + LPS induction of iNOS is modulated by ERK, JNK/SAPK and p38 mapk in a mouse macrophage cell line. *American Journal of Physiology – Cell Physiology*, *280*, C441–C450.

Chelvarajan, R. L., Liu, Y., Popa, D., Getchell, M. L., Getchell, T. V., Stromberg, A. J., et al. (2006). Molecular basis of age-associated cytokine dysregulation in LPS-stimulated macrophages. *Journal of Leukocyte Biology*, *79*, 1314–1327.

Chung, H. T., Pae, H. O., Choi, B. M., Billiar, T. R., & Kim, Y. M. (2001). Nitric oxide as a bioregulator of apoptosis. *Biochemical and Biophysical Research Communications*, *282*, 1075–1079.

Gary, J. L., & Lapadat, R. (2002). Mitogen-activated protein kinase pathways mediated by ERK, JNK, and p38 protein kinases. *Science*, *298*, 1911–1912.

Gerber, J. S., & Mosser, D. M. (2001). Reversing lipopolysaccharide toxicity by ligating the macrophage Fcγ receptors. *Journal of Immunology*, *166*, 6861–6868.

Green, L. C., Wanger, D. A., Glogowski, J., Skipper, P. L., Wishnok, J. S., & Tannenbaum, S. R. (1982). Analysis of nitrate, nitrite, and 15 N nitrate in biological fluids. *Analytical Biochemistry*, *126*, 131–136.

Hakomori, S. E. N. I. (1964). A rapid permethylation of glycolipid, and polysaccharide catalyzed by methylsulfinyl carbanion in dimethyl sulfoxide. *Journal of Biochemistry*, *55*, 205–208.

Hou, R. C., Chen, Y. S., Huang, J. R., & Jeng, K. C. (2006). Cross-linked bromelain inhibits lipopolysaccharide-induced cytokine production involving cellular signaling suppression in rats. *Journal of Agricultural and Food Chemistry*, *54*, 2193–2198.

Hwang, P. A., Chien, S. Y., Chan, Y. L., Lu, M. K., Wu, C. H., Kong, Z. L., et al. (2011). Inhibition of lipopolysaccharide (LPS)-induced inflammatory responses by *Sargassum hemiphyllum* sulfated polysaccharide extract in RAW 264.7 macrophage cells. *Journal of Agricultural and Food Chemistry*, *59*, 2062–2068.

John, M. M., Xie, Q. W., & Nathan, C. (1997). Nitric oxide and macrophage function. *Annual Review of Immunology*, *332*, 323–350.

Kim, Y. H., Lee, S. H., Lee, J. Y., Choi, S. W., Park, J. W., & Kwon, T. K. (2004). Triptolide inhibits murine-inducible nitric oxide synthase expression by down-regulating lipopolysaccharide-induced activity of nuclear factor-κB and c-Jun NH_2-terminal kinase. *European Journal of Pharmacology*, *494*, 1–9.

Lacchini, A. H., Davies, A. J., Mackintosh, D., & Walker, A. J. (2006). Beta-1, 3-glucan modulates PKC signalling in *Lymnaea stagnalis* defence cells: A role for PKC in H_2O_2 production and downstream ERK activation. *Journal of Experimental Biology*, *209*, 4829–4840.

Leung, M., Liu, C., Koon, J., & Fung, K. (2006). Polysaccharide biological response modifiers. *Immunology Letters*, *105*, 101–114.

Liao, C. H., & Lin, J. Y. (2012). Purification, partial characterization and anti-inflammatory characteristics of lotus (*Nelumbo nucifera* Gaertn) plumule polysaccharides. *Food Chemistry*, *135*, 1818–1827.

Lin, Y. L., Liang, Y. C., Lee, S. S., & Chiang, B. L. (2005). Polysaccharide purified from *Ganoderma lucidum* induced activation and maturation of human monocyte-derived dendritic cells by the NF-kappaB and p38 mitogen-activated protein kinase pathways. *Journal of Leukocyte Biology*, *78*, 533–543.

O'Shea, J. J., & Murray, P. J. (2008). Cytokine signaling modules in inflammatory responses. *Immunity*, *28*, 477–487.

Picton, L., Bataille, I., & Muller, G. (2000). Analysis of a complex polysaccharide (gum arabic) by multi-angle laser light scattering coupled on-line to size exclusion chromatography and flow field flow fractionation. *Carbohydrate Polymers*, *42*, 23–31.

Rogers, N. C., Slack, E. C., Edwards, A. D., Nolte, M. A., Schulz, O., Schweighoffer, E., et al. (2005). Syk-dependent cytokine induction by Dectin-1 reveals a novel pattern recognition pathway for C type lectins. *Immunity*, *22*, 507–517.

Tezuka, Y., Imai, K., Oshima, M., & Chiba, T. (1987). Determination of substituent distribution in cellulose ethers by means of a carbon-13 NMR study on their acetylated derivatives, 1. Methylcellulose. *Macromolecules*, *20*, 2413–2418.

Wang, J., Zhang, L., Yu, Y., & Cheung, P. C. (2009). Enhancement of antitumor activities in sulfated and carboxymethylated polysaccharides of *Ganoderma lucidum*. *Journal of Agricultural and Food Chemistry*, *57*, 10565–10572.

Zhang, G., & Ghosh, S. (2001). Toll-like receptor-mediated NF-kappaB activation: A phylogenetically conserved paradigm in innate immunity. *Journal of Clinical Investigation*, *107*, 13–20.